

EXPERIMENTAL DEVICE FOR TESTING OF SEMI-ACTIVE MAGNETORHEOLOGICAL DAMPER

KAREL SEBESTA, JIRI ZACEK, MATUS SALVA

Brno University of Technology,
Faculty of Mechanical Engineering,
Institute of Machine and Industrial Design,
Brno, Czech Republic

DOI: 10.17973/MMSJ.2023_03_2023004

Karel.Sebesta@vutbr.cz

Transmission of vibrations into the cabin while driving and the general comfort of the driver is essential for agricultural and heavy-duty vehicles. Due to long working hours and rough terrain during operation, reduced attention or health problems may occur when significant vibrations are transferred from the vehicle chassis to the driver. One of the modern damping systems which can drastically minimise vibration transmission is the semi-active suspension system featuring a Magnetorheological damper. This damper can adjust the damping level using varying currents through the coil. The advantage of this system is the wide dynamic range and the fast response time of damping force. This paper aims to create a device for testing a S/A controlled fast MR damper in seat suspension, further measuring the effectiveness of the damping system in compare with passive damper.

KEYWORDS

seat scissor mechanism, vibration, magnetorheological damper, semi-active suspension, Sky-Hook

1 INTRODUCTION

In the heavy-duty or agricultural transport sectors, drivers are often forced to work in challenging conditions for many hours. For example, the most common acceleration affecting tractor drivers is 0.5-1.5 G at a frequency of 2-7 Hz (ISO 2631). These unwanted vibrations, with long-term exposure, can result in serious health problems (osteoarthritis, abdominal pain, intestinal disorders) [Choi 2007]. One of the solutions is to improve the damping of the rider's seat, thus reducing the transmission of vibrations. This will give the driver much more comfort, leading to a better focus on work and a higher chance of avoiding health problems. The most common types of seat suspension are passive, which use a spring and a hydraulic damper [Mayton 2014], or to a lesser extent, systems with a pneumatic or hydraulic actuator [Al-Ashmori 2020]. Passive suspension systems cannot reduce vibrations across the entire frequency spectrum. Because passive dampers can only be tuned to a specific frequency spectrum, it is impossible to design a passive system with low peak resonance and appropriate vibration isolation at high frequencies. Active suspension achieves excellent results in shock absorption (use actuators) but at the cost of a more complicated solution and higher energy consumption, which is reflected in the high price [Ning 2016]. A solution could be semi-active (S/A) suspension systems with a Magnetorheological (MR) damper. Dynamic scheme with damping force—piston velocity characteristic is in Fig. 1. These systems set the ideal damping according to sensor

data and thus significantly suppress vibration transmission [Choi 2001]. S/A systems do not require as much electrical power as active ones, achieving equivalent performance in many applications [Machacek 2017].

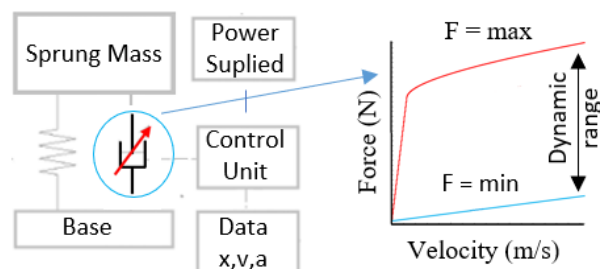


Figure 1. Semi-Active suspension system with detail of Force-velocity characteristic of Magnetorheological damper

MR fluid in a hydraulic tube of a damper contains micro-sized ferromagnetic iron particles. The action of an external magnetic field created by the coil in the damper piston core increases the apparent viscosity of MR fluid and, thus, the damping force. The simplified sketch of an MR damper with essential components and the direction of the magnetic field is in Fig. 2. The fluid flows through the annular orifice in the opposite direction to the movement of the piston.

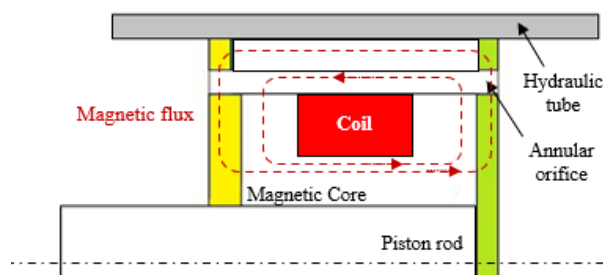


Figure 2. Sketch of MR damper piston group

This advanced technology quickly changes the damping force during operation (units of milliseconds) [Kubik 2017]. The faster the response time of damping force, the better the vibration reduction [Strecker 2015]. MR dampers have a large dynamic range (10-20), which is the ratio between the maximum and minimum force, as shown in Fig. 1. Based on the date of relative velocity and acceleration of sprung mass, the control system changes the input current on the coil so the ideal damping of vibration can be set up. The basic algorithm is ON/OFF [Huang 2012] mode or gradually adjusts of current like the linear Sky-hook [Strecker 2018] algorithm. In the last decade, a whole series of design proposals for MR dampers were published [Yu 2019] [Bai 2017], but much less attention was paid to the construction of test stands and the subsequent tuning of algorithms.

This contribution aims to design a stand for testing the S/A suspension system with a fast response time MR damper and to demonstrate the applicability of this technology in seat damping by reducing the acceleration of the sprung mass and, thus, the comfort of the passenger.

2 STAND FOR TESTING OF SEAT DAMPING WITH MAGNETORHEOLOGICAL DAMPER

2.1 The dynamic model of seat

The dynamic model of the sprung seat mechanism consists of one mass (mass of the seat and a driver) and the base element (testing stand (Fig.3). The base is kinematically excited, and the forces are transmitted via elastic and dampened bonds.

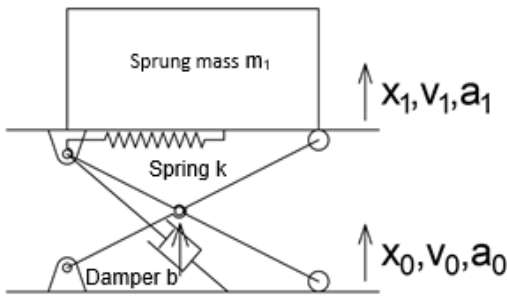


Figure 3. Sketch of the scissor mechanism of the seat

The elastic bond represents the springs with stiffness k . The pretension of the springs can be adjusted. The dampened bond stands in for the semi-active damper (in our case MR damper). The forces of the damper are dependent not only on the damper velocity but its characteristics can also be adjusted on external parameters. The spring and the damper are connected to the spring-mass via the scissor's mechanism levers. The actual forces acting on the seat had to be recalculated according to the mechanism's geometry. To simplify the model, it was decided that the movement of the seat would be modelled in the vertical axis only. The longitudinal movement was considered as not important because the angle of the base changes $\pm 0,4^\circ$ degrees and has minimal effect on acceleration measurements for a sprung mass. The standard dampened system with one mass can be described in Eq 1.

$$m_1 \ddot{x}_1 + b_1 (\dot{x}_1 - \dot{x}_0) + k_1 (x_1 - x_0) = -m_1 g \quad (1)$$

Where m is the mass, x_1 is the position of the mass, x_0 is the position of the base, b is damping coefficient and k is the spring stiffness. Because the scissor mechanism does not transmit the forces linearly (Fig. 3), therefore the system can be described by the following equation (Eq. 2):

$$m_1 \ddot{x}_1 + F_{damping}(I, x_0, x_1, v_{rel}) + F_{elastic}(k, x_0, x_1) = -m_1 g \quad (2)$$

Where $F_{damping}$ is damping force, $F_{elastic}$ is elastic force, v_{rel} means the relative velocity x means the position and I is current, which is sent to the damper, k is a combined spring stiffness ($k = 113,8$ kN/m), m_1 is a mass of 100 kg, and g is gravity acceleration. The $F_{damping}$ parameters varied depending on the used damper. The used F-v characteristics are shown in Fig.4.

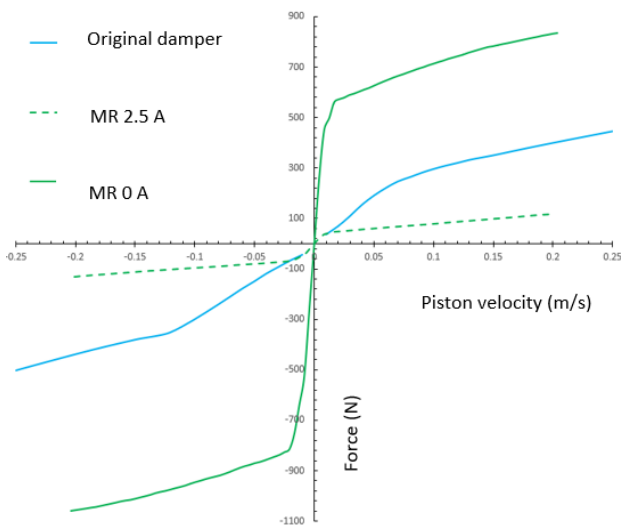


Figure 4. F-V characteristics of the dampers

The algorithms control the damper, which switches the current and determines F-v characteristic. The algorithm, we used in our test, is a two-stage Sky-hook (SH-2), which changes the damping characteristics of the damper according to Eq 3.

$$F_{damping} = \begin{cases} F_{high}, & \text{if } v_1(v_1 - v_0) \geq 0 \\ F_{low}, & \text{if } v_1(v_1 - v_0) < 0 \end{cases} \quad (3)$$

In this equation, v_1 is a velocity of sprung mass, v_0 is a velocity of the base and F is the damping force of the damper. The seat moves only in one direction, the values were treated as scalars.

The system was then programmed in Matlab using a Simulink environment. The simulation was conducted using *ode4* (Runge-Kutta) method with the fixed step of 0.0002 s.

2.2 Experimental device

The diagram of the stand for testing seat damping using an MR damper is in Fig. 5. It is a rectangular welded statically and tilted frame. The electromotor (1.5 kW, 1450 rpm) is placed on the static frame together with the belt transmission (transmission to slow, gear ratio 4.5). The motor is controlled by using a frequency converter. Thus, the shaft speed can range from 0 to 400 rpm. A replaceable eccentric is attached to the shaft using compression sleeves. For experimental verification, an eccentricity of 10 mm is used. These two parameters, therefore, determine the properties of excited vibrations. The scissor mechanism (part of the tested seat) is on a movable frame. In this mechanism are located screw tension springs (for adjusting the zero position according to the weight of the driver) and the original shock absorber, which is replaced with an MR damper based on results from dynamic simulations. The weight of the driver was determined to be 80 kg. Together with the seat, the total weight of the sprung mass was 100 kg. This design was chosen for simplicity and the possibility of easy assembly and transfer.

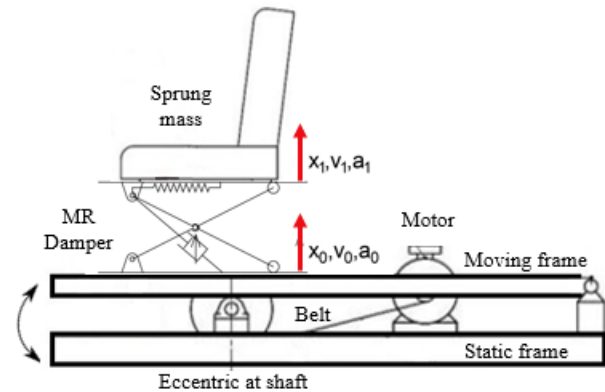


Figure 5. Sketch of testing stand for the seat with MR damper

The overall 3D model is in Fig. 6. The cylindrical weights on the scissor mechanism represent the 100 kg driver. The grey box above the pivot of the tilting frame contains the electronics, the control system, and the power source. The resulting weight of the static frame (1.8 m x 0.8 m) is 250 kg and is firmly bolted to the base plate.

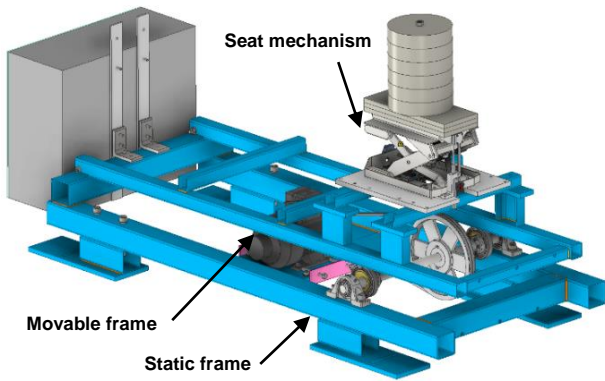


Figure 6. 3D model of testing stand

For reducing of tilting movement of the sprung mass and the most direct measurement of the contribution of MR technology used in the suspension of the seat, the sprung mass was guided by the watt mechanism which ensures translational movement in one axis. In the case of the stand, it was an up-and-down movement of the sprung mass. The assembled stand can be seen in the real assembly of measurement stand Fig. 7.



Figure 7. Stand for testing of S/A suspension system with fast magnetorheological damper

3 MATERIALS AND METHODS

3.1 Measurement chain of stand

Two measuring chains were used for the measurement: the green one and the blue one in Fig. 8. The blue one used piezoelectric accelerometers placed on a sprung mass acc_{B1} (next to the weight) and on an unsprung mass acc_{B0} (at the base of the seat). Furthermore, a position sensor between the seat and the moving frame (relative position) was used to measure the movement X_{B1} . Data from these sensors were processed in the DEWE 800 measuring centre using DeweSoft and Matlab postprocessing in a PC. The blue measurement chain was used during testing mainly for verification of the second (green) measurement chain and for obtaining final results used for calculating transmissibility curves and acceleration of the sprung mass. The second measurement chain (the green one) consisted of a magnetic position sensor X_{A1} between the seat and the moving frame and an accelerometer on top of the seat acc_{A1} . The green chain was used to control the MR damper by current I_A , which was backwards measured by current clamps I_B .

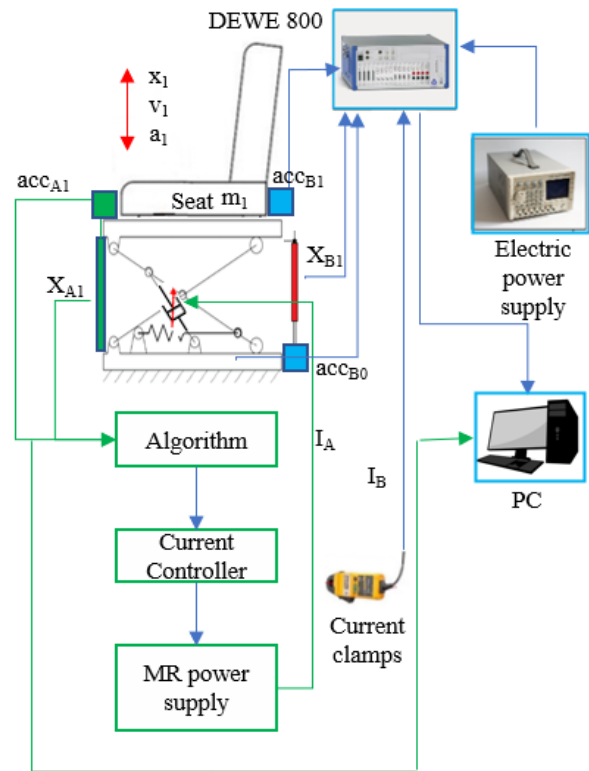


Figure 8. Stand for testing of S/A suspension system with fast Magnetorheological damper

3.2 Damping control system

Values obtained from the measurement chain described in Figure 8 (green) were sent via I_{2C} to the Raspberry Pi Pico microcontroller. To use the input signal in semi-active algorithms, it was necessary to process the signal and use methods such as zero-g offsetting of acceleration and frequency filtering. The parallelisation process was used to ensure a small time delay of semi-active control. The first core was used to read data, process the data and switch the output current depending on the selected semi-active algorithm (Fig. 9 left). The second core is mainly used for communication with the user. It allows the user to switch algorithms and set current values through commands. The second core is also used to print the output values of the measured signal (Fig. 9 right).

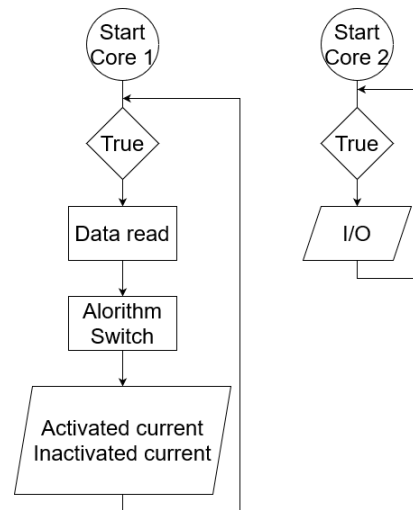


Figure 9. Control logic diagram for CORE 1 (left) and CORE2 (right) for MR damper control

4 RESULTS AND DISCUSSION

4.1 Determining the appropriate damper F-v characteristic

Firstly, it was essential to find an ideal damping characteristic of the damper. The seat was excited by a movement of the base with an amplitude of 10 mm, which frequency was changed during the test by linear sweep from 0 to 3 Hz. The F-v characteristics were designed around: the damper's damping level (b_t), dynamic range, yield stress critical velocity (v_{crit}), and friction (F_t). These parameters can be seen in Fig. 10.

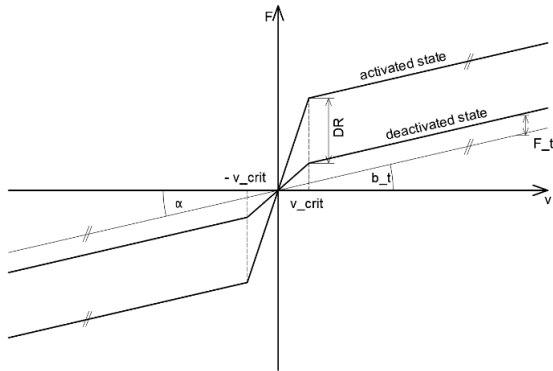


Figure 10. Parameters of F-v characteristics for MR damper selection

A measurement of research group's dampers was found that the frictional force tends to be constant during most of its F-v characteristics. The main source of parasitic frictional forces are seals (especially piston rod seal) and piston guides. According to measurements, the conservative value of $F_t = 50$ N was chosen. The measurements also showed that the piston velocity (v_{crit}), where the F-v curve changes its inclination, is around 0.02 m/s. Those parameters were used for all simulations. It was found that the ideal damper should have a damping level around $b_t = 200$ Nm/s and a dynamic range of 7. The main criterion used for evaluating damping efficiency was the transmissibility curve, which was obtained from FFT of both sprung and unsprung bodies. According to the simulated parameters, an ideal MR damper was selected from the research group's stock. Selected damper has response time τ_{63} 4 ms.

4.2 Comparison of the current switching

To determine the best performance of the semi-active control, several issues of measured signal data were necessary to overcome. For optimal control, the input signal should be smooth (without parasitic frequencies) and with the minor delay possible. Fig. 11 shows that acceleration of sprung mass with the used low pass filter at 1000 Hz (due to aliasing) contains parasitic frequencies at 30 Hz to 130 Hz. It is caused by insufficient stiffness of the seat mechanism and the clearances in the pivots and guides. It is possible to overcome this issue using a lowpass filter at lower frequencies. It significantly improves signal smoothness but causes a time delay of about 8.5 ms.

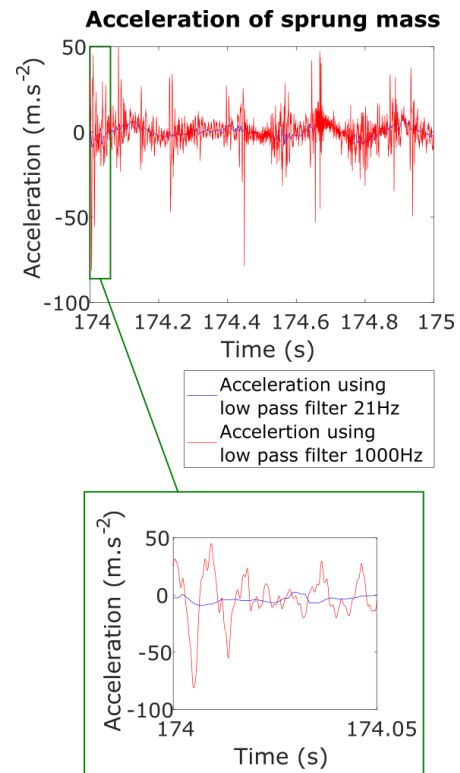


Figure 11. Date of acceleration in time with detail

Zero-g offsetting of the acceleration was used to remove static gravity acceleration measured by the used accelerometer. As inputs to Sky-hook algorithm, the velocity of the sprung mass (obtained by integration of acceleration) together with relative velocity (obtained by derivation of the relative position between unsprung mass and sprung mass) were used. As is shown in Figure 12, velocity of the sprung mass contains a small offset caused by used zero-g offsetting methods. Filtering delay mainly causes late switching off the current from activated state to inactivated state.

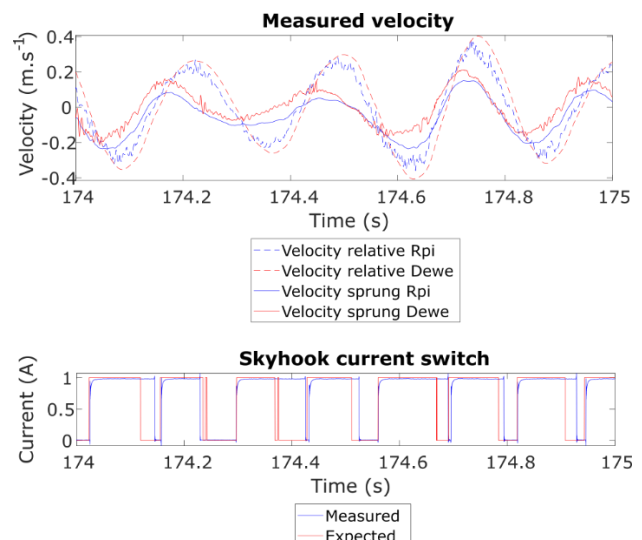


Figure 12. Date of acceleration in time with detail

This undesirable effect can be overcome by using the accelerometer with integrated zero-g offset or by advanced techniques of zero-g offsetting. For the verification of the function Sky-hook algorithm in real seat mechanism, this issue can be neglected and minimised in future work.

4.3 Comparison of simulation and measurement

The aforementioned damping regimes were tested and simulated. The simulation proved that the S/A driven damper shows an improvement in damping compared to the passive regime, as shown in Fig 13. The SH-2 algorithm ought to dampen the seat better, especially in the region of natural frequencies of the seat.

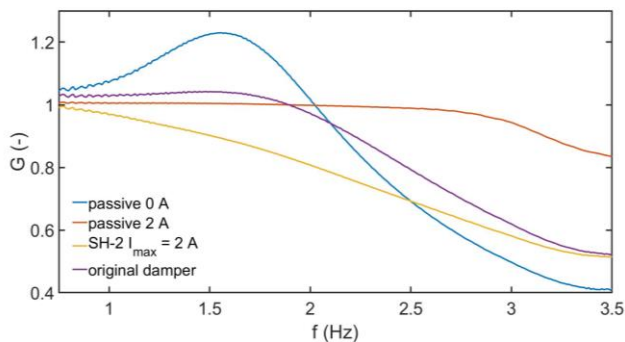


Figure 13. Simulated response characteristics

Those results were confirmed by the measurements in Fig 14. It can be seen that the advantage of the SH-2 algorithm. However, it is not as profound in the natural frequency region as the simulation shows. A lower excitation level combined with the passive friction probably causes this and restrained the damping advantages at natural frequencies.

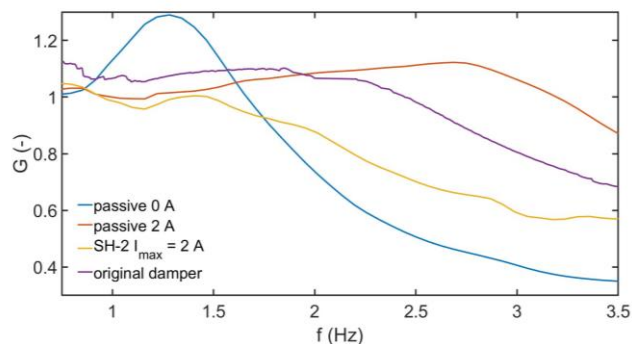


Figure 14 Measured response characteristics

The passive regimes shows that on-state damper ($I = 2 A$) has a very high damping level. The simulation trends match the measurements, which, however, show surprisingly high response characteristics. This could be explained by the lever mechanism's stiffness, which could have been insufficient. This could create undesirable movements (which would be otherwise dampened or transmitted elsewhere) that did probably hold the response characteristics above 1 to almost 3 Hz. The switched off state of MR damper (0 A) showed a low damping level, which was not as profound as it could be due to the passive frictional forces. The original damper was also relatively stiff and did not prove to have ideal characteristics to dampen the seat.

5 CONCLUSIONS

The contribution deals with designing an experimental device for applying a S/A controlled fast MR damper in the seat. Two rectangular welded frames are used for the experimental apparatus. A motor with a frequency converter and a belt transmission generates excitation with constant amplitude (10mm) and variable frequency up to 450 rpm. An acceleration sensor on a sprung mass and a magnetic tape were used to

determine the relative position. The SH-2 algorithm was tested. These tests showed a reduction in the acceleration of the sprung mass in comparison with the original hydraulic shock absorber. This can have health benefits for drivers in long-term exposure of vibration in heavy-duty vehicles. The differences between the model and measurement can be seen in the filtering of the signal and subsequent control of the MR damper based on this data. Part of the seat's scissor mechanism is two rods and four sliding bearings in the guides, whose passive friction is significant compared to the non-activated damping force. So there was an effort to reduce this friction:

- Replacing the bearings in the bases of the scissor mechanism,
- greasing all moving surfaces,
- creating new sliding bushings for the lower shaft
- working with the maximum realistic repulsed mass to reduce the ratio between friction force and load force.

5.1 Subsequent work

As part of the subsequent investigation, a sensitivity analysis of testing stand to the passenger's weight and changes in the eccentric size is assumed. It is also necessary to work more into the functionality of the Sky-hook, where under ideal conditions, it does not switch very well, which is caused by imperfect signal filtering. The other algorithms, such as Acceleration Driven Damper (ADD) or Skyhook Linear (SH-L) should be tested. Another improvement is offered in reducing the friction of the scissor mechanism. A more detailed description of friction in the dynamic model and determination of its influence on the behaviour of the S/A controlled MR damper.

ACKNOWLEDGMENTS

Funding: Grant 7659 "Improving Seat Comfort by semi-Active Control of Magnetorheological Damper" was realised within the project of Quality Internal Grants of the BUT (KInG BUT), Reg. No. CZ.02.2.69/0.0/0.0/19_073/0016948, which was financed from the OP RDE.

REFERENCES

- [Al-Ashmori 2020] Al-Ashmori, Mohammed, and Xu Wang. 2020. "A Systematic Literature Review of Various Control Techniques for Active Seat Suspension Systems." *Applied Sciences (Switzerland)* 10 (3). <https://doi.org/10.3390/app10031148>.
- [Bai 2017] Bai, Xian Xu, Peng Jiang, and Li Jun Qian. 2017. "Integrated Semi-Active Seat Suspension for Both Longitudinal and Vertical Vibration Isolation." *Journal of Intelligent Material Systems and Structures* 28 (8): 1036–49. <https://doi.org/10.1177/1045389X16666179>.
- [Choi 2001] Choi, S. B., M. H. Nam, and B. K. Lee. 2001. "Vibration Control of an MR Seat Damper for Commercial Vehicles." *Journal of Intelligent Material Systems and Structures* 11 (12): 936–44. <https://doi.org/10.1106/AERG-3QKV-31V8-F250>.
- [Choi 2007] Choi, Seung Bok, and Young Min Han. 2007. "Vibration Control of Electrorheological Seat Suspension with Human-Body Model Using Sliding Mode Control." *Journal of Sound and Vibration* 303 (1–2): 391–404. <https://doi.org/10.1016/j.jsv.2007.01.027>.
- [Huang 2012] Huang, Lin, and Xue gong Huang. 2012. "Resistance to Impact Load Analysis of a Novel

Magnetorheological Damper." *Applied Mechanics and Materials* 236–237: 443–47. <https://doi.org/10.4028/www.scientific.net/AMM.236-237.443>.

[Kubik 2017] Kubik, Michal, Ondrej Machacek, Zbynek Strecker, Jakub Roupec, and Ivan Mazurek. 2017. "Design and Testing of Magnetorheological Valve with Fast Force Response Time and Great Dynamic Force Range." *Smart Materials and Structures* 26 (4): 1–9. <https://doi.org/https://doi.org/10.1088/1361-665X/aa6066> Technical.

[Machacek 2017] Machacek, Ondrej, Michal Kubik, and Petr Novak. 2017. "A New Method of Magnetorheological Damper Quality Evaluation." *Engineering Mechanics 2017*, no. May: 594–97.

[Mayton 2014] Mayton, Alan G., Joseph P. DuCarme, Christopher C. Jobes, and Timothy J. Matty. 2006. "Laboratory Investigation of Seat Suspension Performance during Vibration Testing." *American Society of Mechanical Engineers, Design Engineering Division (Publication) DE*, no. May 2014. <https://doi.org/10.1115/IMECE2006-14146>.

[Ning 2016] Ning, Donghong, Shuaishuai Sun, Jiawei Zhang, Haiping Du, Weihua Li, and Xu Wang. 2016. "An Active Seat

Suspension Design for Vibration Control of Heavy-Duty Vehicles." *Journal of Low-Frequency Noise Vibration and Active Control* 35 (4): 264–78. <https://doi.org/10.1177/0263092316676389>.

[Strecker 2015] Strecker, Zbynek, Ivan Mazurek, Jakub Roupec, and Milan Klapka. 2015. "Influence of MR Damper Response Time on Semiactive Suspension Control Efficiency." *Meccanica* 50 (8): 1949–59. <https://doi.org/10.1007/s11012-015-0139-7>.

[Strecker 2018] Strecker, Zbynek, Jakub Roupec, Ivan Mazurek, Ondrej Machacek, and Michal Kubík. 2018. "Influence of Response Time of Magnetorheological Valve in Skyhook Controlled Three-Parameter Damping System." *Advances in Mechanical Engineering* 10 (11): 168781401881119. <https://doi.org/10.1177/1687814018811193>.

[Yu 2019] Yu, Jianqiang, Xiaomin Dong, Zonglun Zhang, and Pinggen Chen. 2019. "A Novel Scissor-Type Magnetorheological Seat Suspension System with Self-Sustainability." *Journal of Intelligent Material Systems and Structures* 30 (5): 665–76. <https://doi.org/10.1177/1045389X17754256>.

CONTACTS:

Ing. Karel Sebesta
Brno University of Technology
Faculty of Mechanical Engineering
Institute of Machine and Industrial Design
Technická 2896/2, 616 69 Brno, Czech Republic
Email: Karel.Sebesta@vutbr.cz